Supporting Information: Accurate Quasiparticle Spectra from the T-matrix Self Energy and the Particle-Particle Random Phase Approximation

Du Zhang,† Neil Qiang Su,† and Weitao Yang*,†,‡

†*Department of Chemistry, Duke University, Durham, NC 27708*

‡*Key Laboratory of Theoretical Chemistry of Environment, School of Chemistry and Environment, South China Normal University, Guangzhou 510006, China*

E-mail: weitao.yang@duke.edu

Derivation of the working equation for the T-matrix self energy approximation

The second-order self energy

In the section, we review the first-order self energy terms (using the bare Coulomb interactions). The direct Hartree term is given as follows.

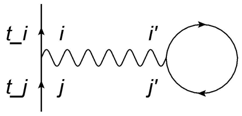

Figure 0.1: Diagrammatic representation of $\Sigma_{ij}^{(1)-d}(t_i - t_j)$

The algebraic expression is given by

$$
\begin{aligned}
&\Sigma_{ij}^{(1)-d}(t_i - t_j)\\
=&(-1)i\sum_{i'j'}\langle ii'|jj'\rangle G_{j'i'}(t_i - t_j)\delta(t_i^+, t_j)\\
=&(-1)i\sum_{i'j'}\langle ii'|jj'\rangle(-i)\langle\Psi_0^N|\hat{T}[\hat{a}_{j'}(t_j)\hat{a}_{i'}^\dagger(t_j^+)]|\Psi_0^N\rangle\delta(t_i^+, t_j)\\
=&\sum_{i'j'}\langle ii'|jj'\rangle\langle\Psi_0^N|\hat{a}_{i'}^\dagger(t_j^+)\hat{a}_{j'}(t_j)|\Psi_0^N\rangle\delta(t_i^+, t_j)\\
=&\sum_{i'j'}\delta(t_i^+, t_j)\langle ii'|jj'\rangle\rho_{j'i'}\\
=&(-1)i\sum_{k_1k_3}\langle ik_3|jk_1\rangle G_{k_1k_3}(t_i - t_j)\delta(t_i^+, t_j)\\
=&(-1)i\sum_{k_1k_3}\langle ij|\bar{V}^{ph}|k_1k_3\rangle G_{k_1k_3}(t_i - t_j)\delta(t_i^+, t_j),
\end{aligned}
\tag{0.1}
$$

where the notation $\bar{V}^{ph}$ is given in[1]. And the Fock exchange term is given as follows.

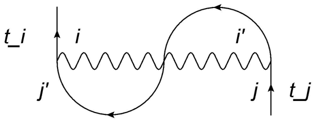

Figure 0.2: Diagrammatic representation of $\Sigma_{ij}^{(1)-x}(t_i - t_j)$

The algebraic expression is given by

$$\begin{aligned}
&\Sigma_{ij}^{(1)-x}(t_i - t_j) \\
=&i \sum_{i'j'} \langle ii'|j'j\rangle G_{j'i'}(t_i - t_j)\delta(t_i^+, t_j) \\
=&-\sum_{i'j'} \delta(t_i^+, t_j)\langle ii'|j'j\rangle \rho_{j'i'} \\
=&i \sum_{k_1k_3} \langle ik_3|k_1j\rangle G_{k_1k_3}(t_i - t_j)\delta(t_i^+, t_j) \\
=&i \sum_{k_1k_3} \langle ik_1|\bar{V}^{ph}|jk_3\rangle G_{k_1k_3}(t_i - t_j)\delta(t_i^+, t_j).
\end{aligned} \tag{0.2}$$

For the second order, let us examine the following diagrammatic representation below.

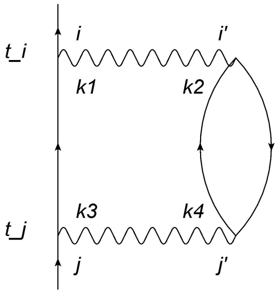

Figure 0.3: Diagrammatic representation of $\Sigma_{ij}^{(2)}(t_i - t_j)$

Interpreting the wiggled lines as antisymmetrized Coulomb interactions, the analytic expression is given by

$$\begin{aligned}
&\Sigma_{ij}^{(2)}(t_i - t_j) \\
=&\frac{1}{2}(-1)i^2 \sum_{i'j'k_1k_2k_3k_4} \langle ii'||k_1k_2\rangle\langle k_3k_4||jj'\rangle G_{k_1k_3}(t_i - t_j)G_{k_2k_4}(t_i - t_j)G_{j'i'}(t_j - t_i).
\end{aligned} \tag{0.3}$$

Or interpreting the wiggled lines as bare Coulomb interactions, the analytic expression is given by,

$$\begin{aligned}&\Sigma_{ij}^{(2)-d}(t_i-t_j)\\ =&(-1)i^2\sum_{i'j'k_1k_2k_3k_4}\langle ii'|k_1k_2\rangle\langle k_3k_4|jj'\rangle G_{k_1k_3}(t_i-t_j)G_{k_2k_4}(t_i-t_j)G_{j'i'}(t_j-t_i),\end{aligned}\tag{0.4}$$

containing only the direct contribution.

The ph RPA and the corresponding GW approximation

In the section, we review the implementation of GW from the ph-RPA perspective[1]. We may define the independent quasiparticle part of the particle-hole channel four-point polarization function,

$$\chi^{IQP}_{k_2i',k_4j'}(t_i-t_j)=-iG_{k_2k_4}(t_i-t_j)G_{j'i'}(t_j-t_i),\tag{0.5}$$

and the two-electron integral notation[1],

$$\langle ik_1|\bar{V}^{ph}|k_2i'\rangle=\langle ii'|k_1k_2\rangle,\tag{0.6}$$

$$\langle k_3j|\bar{V}^{ph}|j'k_4\rangle=\langle k_3k_4|jj'\rangle=\langle k_4j'|\bar{V}^{ph}|jk_3\rangle.\tag{0.7}$$

Thus the second-order self energy expressions become

$$\begin{aligned}&\Sigma_{ij}^{(2)}(t_i-t_j)\\ =&\frac{i}{2}\sum_{i'j'k_1k_2k_3k_4}\langle ik_1|V^{ph}|k_2i'\rangle\chi^{IQP}_{k_2i',k_4j'}(t_i-t_j)\langle k_4j'|V^{ph}|jk_3\rangle G_{k_1k_3}(t_i-t_j),\end{aligned}\tag{0.8}$$

$$\begin{aligned}&\Sigma_{ij}^{(2)-d}(t_i-t_j)\\ =&i\sum_{i'j'k_1k_2k_3k_4}\langle ik_1|\bar{V}^{ph}|k_2i'\rangle\chi^{IQP}_{k_2i',k_4j'}(t_i-t_j)\langle k_4j'|\bar{V}^{ph}|jk_3\rangle G_{k_1k_3}(t_i-t_j).\end{aligned}\tag{0.9}$$

Now defining the following quantity

$$\langle ik_1|\bar{W}^{ph}(t_i-t_j)|jk_3\rangle = \langle ik_1|\bar{V}^{ph}|jk_3\rangle\delta(t_i^+,t_j)+\sum_{k_2i'k_4j'}\langle ik_1|\bar{V}^{ph}|k_2i'\rangle\chi_{k_2i',k_4j'}(t_i-t_j)\langle k_4j'|\bar{V}^{ph}|jk_3\rangle, \tag{0.10}$$

where

$$\chi = \chi^{IQP} + \chi^{IQP}\bar{V}^{ph}\chi. \tag{0.11}$$

the GW self energy thus becomes

$$\begin{aligned}&\Sigma^{GW}_{ij}(t_i-t_j)\\ =&(-1)i\sum_{k_1k_3}\langle ij|\bar{V}^{ph}|k_1k_3\rangle G_{k_1k_3}(t_i-t_j)\delta(t_i^+,t_j)+i\sum_{k_1k_3}\langle ik_1|\bar{W}^{ph}(t_i-t_j)|jk_3\rangle G_{k_1k_3}(t_i-t_j).\end{aligned} \tag{0.12}$$

In particular, Equation (0.12) is known as the GW approximation. In the real-space representation, the screened Coulomb interaction becomes

$$\begin{aligned}\bar{W}^{ph}(1,2) =&v(1,2)+\int d34 v(1,3)\chi(3,4)v(4,2)\\ =&v(x_1,x_2)\delta(t_1^+,t_2)+\int dx_3dx_4 v(x_1,x_3)\chi(x_3t_1,x_4t_2)v(x_4,x_2),\end{aligned} \tag{0.13}$$

and the xc part of the self energy becomes

$$\Sigma^{xc-GW}(1,2) = iG(1,2)\bar{W}^{ph}(1,2). \tag{0.14}$$

The G_0W_0 approximation is obtained when the non-interacting G_0 is used in place of the interacting G and the W matrix is replaced by W_0 obtained with the ph-RPA.

The pp-RPA and the corresponding T-matrix approximation

Now considering it from the pp-RPA perspective, we define the independent quasiparticle part of the pairing channel four-point polarization function,

$$\begin{aligned}&K^{IQP}_{k_1k_2,k_3k_4}(t_i-t_j)\\=&i\left[G_{k_1k_3}(t_i-t_j)G_{k_2k_4}(t_i-t_j)-G_{k_1k_4}(t_i-t_j)G_{k_2k_3}(t_i-t_j)\right],\end{aligned}\tag{0.15}$$

and the two-electron integral notation,

$$\langle ii'|V^{pp}|k_1k_2\rangle=\langle ii'||k_1k_2\rangle,\tag{0.16}$$

$$\langle k_3k_4|V^{pp}|jj'\rangle=\langle k_3k_4||jj'\rangle.\tag{0.17}$$

Replacing the interacting G with the non-interacting G_0, we recover

$$\begin{aligned}&K^{0}_{k_1k_2,k_3k_4}(t_i-t_j)\\=&i\left[\left(G_0\right)_{k_1k_3}(t_i-t_j)\left(G_0\right)_{k_2k_4}(t_i-t_j)-\left(G_0\right)_{k_1k_4}(t_i-t_j)\left(G_0\right)_{k_2k_3}(t_i-t_j)\right]\end{aligned}\tag{0.18}$$

defined in[2]. Thus

$$\begin{aligned}&\Sigma^{(2)}_{ij}(t_i-t_j)\\=&\frac{1}{2}(-1)i^2\sum_{i'j'k_1k_2k_3k_4}\langle ii'|V^{pp}|k_1k_2\rangle\langle k_3k_4|V^{pp}|jj'\rangle G_{k_1k_3}(t_i-t_j)G_{k_2k_4}(t_i-t_j)G_{j'i'}(t_j-t_i)\\=&\frac{1}{4}(-1)i^2\sum_{i'j'k_1k_2k_3k_4}\langle ii'|V^{pp}|k_1k_2\rangle\langle k_3k_4|V^{pp}|jj'\rangle G_{k_1k_3}(t_i-t_j)G_{k_2k_4}(t_i-t_j)G_{j'i'}(t_j-t_i)\\+&\frac{1}{4}(-1)i^2\sum_{i'j'k_1k_2k_3k_4}\langle ii'|V^{pp}|k_1k_2\rangle\langle k_4k_3|V^{pp}|jj'\rangle G_{k_1k_4}(t_i-t_j)G_{k_2k_3}(t_i-t_j)G_{j'i'}(t_j-t_i)\\=&\frac{1}{4}(-1)i\sum_{i'j'k_1k_2k_3k_4}\langle ii'|V^{pp}|k_1k_2\rangle K^{IQP}_{k_1k_2,k_3k_4}(t_i-t_j)\langle k_3k_4|V^{pp}|jj'\rangle G_{j'i'}(t_j-t_i).\end{aligned}\tag{0.19}$$

Now remembering that

$$\begin{aligned}&\Sigma^{(1)}_{ij}(t_i-t_j)\\=&(-1)i\sum_{i'j'}\langle ii'|V^{pp}|jj'\rangle G_{j'i'}(t_j-t_i)\delta(t_i,t_j^+),\end{aligned}\tag{0.20}$$

which we wrote differently than we did for the ph RPA case in Equations (0.1) and (0.2). In a similar fashion to the definition of the ph channel screened interaction $\bar{W}^{ph}$ (Equation (0.10)) in terms of the bare Coulomb interaction and the ph response, we now define

$$\begin{aligned}&\langle ii'|W^{pp}(t_i-t_j)|jj'\rangle\\=&\langle ii'|V^{pp}|jj'\rangle\delta(t_i,t_j^+)+\frac{1}{4}\sum_{k_1k_2k_3k_4}\langle ii'|V^{pp}|k_1k_2\rangle K_{k_1k_2,k_3k_4}(t_i-t_j)\langle k_3k_4|V^{pp}|jj'\rangle,\end{aligned}\tag{0.21}$$

where

$$K=K^0+\frac{1}{4}K^0V^{pp}K.\tag{0.22}$$

Thus the pp-RPA self energy is given by

$$\Sigma^T_{ij}(t_i-t_j)=(-1)i\sum_{i'j'}\langle ii'|W^{pp}(t_i-t_j)|jj'\rangle G_{j'i'}(t_i-t_j).\tag{0.23}$$

Compare this with the real-space expression[3],

$$\Sigma^T(x_1t_1,x_2t_2)=i\int dt_3\int dt_4\int dx_3\int dx_4G(x_4t_4,x_3t_3)T(x_1t_1,x_3t_3;x_2t_2,x_4t_4),\tag{0.24}$$

it is clear that the orbital space expression W^{pp} and the real-space expression T, also known as the T matrix, differ only by a negative sign. In the orbital space representation, we have

$$\begin{aligned}&T_{ii',jj'}(t_i,t_{i'};t_j,t_{j'})\\=&-\langle ii'|W^{pp}(t_i-t_j)|jj'\rangle\delta(t_i,t_{i'})\delta(t_j,t_{j'}).\end{aligned}\tag{0.25}$$

The pp channel counterpart for the G_0W_0 approximation is recovered when the non-interacting G_0 is used in place of the interacting G and the T matrix is replaced by T_0 obtained with the pp-RPA.

Working equations for the quasiparticle correction implementation

Now we shall restrict ourselves to the non-self-consistent G_0W_0 and T-matrix approximations.

The ph case

This part provides a self-containing review of the ph case. It is compiled and adapted from multiple references[1,4–7].

The screened interaction now takes the adiabatic ph-RPA/TDDFT response,

$$\begin{aligned}\bar{W}^{ph}(1,2) =& v(1,2) + \int d34 v(1,3)\chi(3,4)v(4,2) \\ =& v(x_1,x_2)\delta(t_1^+,t_2) + \int dx_3 dx_4 v(x_1,x_3)\chi(x_3t_1,x_4t_2)v(x_4,x_2),\end{aligned} \tag{0.26}$$

where

$$\chi = \chi^{KS} + \chi^{KS} f_{Hxc}\chi, \tag{0.27}$$

is obtained from a ph-RPA/ATDDFT calculation. The xc self energy expression is given by

$$\Sigma^{xc-G_0W_0}(1,2) = iG^{KS}(1,2)\bar{W}^{ph}(1,2). \tag{0.28}$$

Performing the Fourier transform into the frequency domain, the self energy expression becomes

$$\begin{aligned}
\Sigma^{xc-G_0W_0}(x_1,x_2|\omega) =& i\int d(t_1-t_2)e^{i\omega(t_1-t_2)}G^{KS}(x_1,x_2|t_1-t_2)\bar{W}^{ph}(x_1,x_2|t_1-t_2) \\
=& i\int d(t_1-t_2)e^{i\omega(t_1-t_2)}G^{KS}(x_1,x_2|t_1-t_2)\int dt'\delta(t',t_1-t_2)\bar{W}^{ph}(x_1,x_2|t') \\
=& i\int d(t_1-t_2)e^{i\omega(t_1-t_2)}G^{KS}(x_1,x_2|t_1-t_2)\int dt'\int\frac{d\omega'}{2\pi}e^{i\omega'(t'-t_1+t_2)}\bar{W}^{ph}(x_1,x_2|t') \\
=& -\int\frac{d\omega'}{2\pi i}\int d(t_1-t_2)e^{i(\omega-\omega')(t_1-t_2)}G^{KS}(x_1,x_2|t_1-t_2)\int dt'e^{i\omega't'}\bar{W}^{ph}(x_1,x_2|t') \\
=& -\int\frac{d\omega'}{2\pi i}G^{KS}(x_1,x_2|\omega-\omega')\bar{W}^{ph}(x_1,x_2|\omega').
\end{aligned} \tag{0.29}$$

Particularly, the Fourier transform of $\delta(t_1^+,t_2)$ is given by

$$\begin{aligned}
&\int d(t_1-t_2)e^{i\omega(t_1-t_2)}\delta(t_1^+,t_2) \\
=&\int d(t_1-t_2)e^{i\omega(t_1-t_2)}\int\frac{d\omega'}{2\pi}e^{i\omega'(t_1-t_2)}e^{i\omega'\eta} \\
=&\int d\omega' e^{i\omega'\eta}\int\frac{d(t_1-t_2)}{2\pi}e^{i(\omega+\omega')(t_1-t_2)} \\
=&\int d\omega' e^{i\omega'\eta}\delta(\omega,-\omega') \\
=&e^{-i\omega\eta},
\end{aligned} \tag{0.30}$$

where η is a positive infinitesimal. Therefore in the frequency domain the screened Coulomb interaction is given by

$$\bar{W}^{ph}(x_1,x_2|\omega) = v(x_1,x_2)e^{-i\omega\eta} + \int dx_3dx_4v(x_1,x_3)\chi(x_3,x_4|\omega)v(x_4,x_2). \tag{0.31}$$

The Lehmann representation of the Kohn-Sham one-particle Green's function is given by

$$G^{KS}(x_1,x_2|\omega) = \sum_a\frac{\phi_a(x_1)\phi_a^*(x_2)}{\omega-\epsilon_a+i\eta} + \sum_i\frac{\phi_i(x_1)\phi_i^*(x_2)}{\omega-\epsilon_i-i\eta}. \tag{0.32}$$

Thus the so-called exchange part of the self energy is given by

$$
\begin{aligned}
&\Sigma^{x-G_0W_0}(x_1, x_2|\omega) \\
=&-\int \frac{d\omega'}{2\pi i} G^{KS}(x_1, x_2|\omega-\omega') v(x_1, x_2) e^{-i\omega'\eta} \\
=&-\int \frac{d\omega'}{2\pi i} \left(\sum_a \frac{\phi_a(x_1)\phi_a^*(x_2)}{\omega-\omega'-\epsilon_a+i\eta} + \sum_i \frac{\phi_i(x_1)\phi_i^*(x_2)}{\omega-\omega'-\epsilon_i-i\eta} \right) v(x_1, x_2) e^{-i\omega'\eta} \\
=&\int \frac{d\omega'}{2\pi i} \left(\sum_i \frac{\phi_i(x_1)\phi_i^*(x_2)}{\omega'-\omega+\epsilon_i+i\eta} + \sum_a \frac{\phi_a(x_1)\phi_a^*(x_2)}{\omega'-\omega+\epsilon_a-i\eta} \right) v(x_1, x_2) e^{-i\omega'\eta} \\
=&-\sum_i \phi_i(x_1)\phi_i^*(x_2) v(x_1, x_2) \\
=&-\frac{\rho(x_1, x_2)}{r_{12}},
\end{aligned}
\tag{0.33}
$$

where the contour integration is performed around the lower-half-plane because of the factor $e^{-i\omega'\eta}$. This recovers the Fock exchange.

Now to consider the correlation part of the self energy $\Sigma^{c-G_0W_0}(x_1, x_2|\omega)$, we need the Lehmann representation for the density-density response function,

$$
\begin{aligned}
&\chi(x_3, x_4|\omega) \\
=&\sum_{m\neq 0} \frac{\rho_m(x_3)\rho_m^*(x_4)}{\omega-\omega_m+i\eta} - \sum_{m\neq 0} \frac{\rho_m(x_4)\rho_m^*(x_3)}{\omega+\omega_m-i\eta},
\end{aligned}
\tag{0.34}
$$

where $\rho_m(x_3) = \langle\Psi_0|\hat{\rho}(x_3)|\Psi_m\rangle = \langle\Psi_0|\hat{\psi}^\dagger(x_3)\hat{\psi}(x_3)|\Psi_m\rangle$. Therefore the correlation part of the self energy is given by

$$
\begin{aligned}
&\Sigma^{c-G_0W_0}(x_1,x_2|\omega)\\
=&-\int\frac{d\omega'}{2\pi i}G^{KS}(x_1,x_2|\omega-\omega')\int dx_3dx_4v(x_1,x_3)\chi(x_3,x_4|\omega')v(x_4,x_2)\\
=&-\int\frac{d\omega'}{2\pi i}\Bigg(\sum_a\frac{\phi_a(x_1)\phi_a^*(x_2)}{\omega-\omega'-\epsilon_a+i\eta}+\sum_i\frac{\phi_i(x_1)\phi_i^*(x_2)}{\omega-\omega'-\epsilon_i-i\eta}\Bigg)\\
&\int dx_3dx_4v(x_1,x_3)\Bigg(\sum_{m\neq 0}\frac{\rho_m(x_3)\rho_m^*(x_4)}{\omega'-\omega_m+i\eta}-\sum_{m\neq 0}\frac{\rho_m(x_4)\rho_m^*(x_3)}{\omega'+\omega_m-i\eta}\Bigg)v(x_4,x_2)\\
=&\int dx_3dx_4v(x_1,x_3)v(x_4,x_2)\int\frac{d\omega'}{2\pi i}\Bigg(\sum_i\frac{\phi_i(x_1)\phi_i^*(x_2)}{\omega'-\omega+\epsilon_i+i\eta}+\sum_a\frac{\phi_a(x_1)\phi_a^*(x_2)}{\omega'-\omega+\epsilon_a-i\eta}\Bigg)\\
&\Bigg(\sum_{m\neq 0}\frac{\rho_m(x_3)\rho_m^*(x_4)}{\omega'-\omega_m+i\eta}-\sum_{m\neq 0}\frac{\rho_m(x_4)\rho_m^*(x_3)}{\omega'+\omega_m-i\eta}\Bigg)\\
=&\int dx_3dx_4v(x_1,x_3)v(x_4,x_2)\\
&\Bigg\{\sum_{m\neq 0}\sum_a\Bigg(\frac{\phi_a(x_1)\phi_a^*(x_2)\rho_m(x_3)\rho_m^*(x_4)}{\omega-\epsilon_a-\omega_m+i\eta}-\frac{\phi_a(x_1)\phi_a^*(x_2)\rho_m(x_4)\rho_m^*(x_3)}{\omega-\epsilon_a+i\eta+\omega_m-i\eta}\Bigg)\\
-&\sum_{m\neq 0}\Bigg(\sum_i\frac{\phi_i(x_1)\phi_i^*(x_2)\rho_m(x_4)\rho_m^*(x_3)}{-\omega_m-\omega+\epsilon_i+i\eta}+\sum_a\frac{\phi_a(x_1)\phi_a^*(x_2)\rho_m(x_4)\rho_m^*(x_3)}{-\omega_m+i\eta-\omega+\epsilon_a-i\eta}\Bigg)\Bigg\}\\
=&\int dx_3dx_4v(x_1,x_3)v(x_4,x_2)\\
&\sum_{m\neq 0}\Bigg(\sum_a\frac{\phi_a(x_1)\phi_a^*(x_2)\rho_m(x_3)\rho_m^*(x_4)}{\omega-\epsilon_a-\omega_m+i\eta}+\sum_i\frac{\phi_i(x_1)\phi_i^*(x_2)\rho_m(x_4)\rho_m^*(x_3)}{\omega-\epsilon_i+\omega_m-i\eta}\Bigg).
\end{aligned}
\tag{0.35}
$$

Therefore, the diagonal elements of the correlation part of the self energy is given by

$$
\begin{aligned}
&\Sigma_c^{G_0W_0}(n,n;\omega) \\
=&\int dx_1dx_2\phi_n^*(x_1)\Sigma^{c-G_0W_0}(x_1,x_2|\omega)\phi_n(x_2) \\
=&\int dx_1dx_2dx_3dx_4\phi_n^*(x_1)\phi_n(x_2)v(x_1,x_3)v(x_4,x_2) \\
&\sum_{m\neq 0}\left(\sum_a \frac{\phi_a(x_1)\phi_a^*(x_2)\rho_m(x_3)\rho_m^*(x_4)}{\omega-\epsilon_a-\omega_m+i\eta}+\sum_i \frac{\phi_i(x_1)\phi_i^*(x_2)\rho_m(x_4)\rho_m^*(x_3)}{\omega-\epsilon_i+\omega_m-i\eta}\right) \\
=&\sum_{m\neq 0}\left[\sum_a \frac{(na|\rho_m)(\rho_m|na)}{\omega-\epsilon_a-\omega_m+i\eta}+\sum_i \frac{(\rho_m|in)(in|\rho_m)}{\omega-\epsilon_i+\omega_m-i\eta}\right],
\end{aligned}
\tag{0.36}
$$

where we defined the integrals

$$(na|\rho_m)=\int dxdx'\phi_n^*(x)\phi_a(x)\frac{1}{|r-r'|}\rho_m(x'), \tag{0.37}$$

$$(\rho_m|na)=\int dxdx'\rho_m^*(x)\frac{1}{|r-r'|}\phi_n(x')\phi_a^*(x')=(na|\rho_m)^*. \tag{0.38}$$

Thus

$$\Sigma_c^{G_0W_0}(n,n;\omega)=\sum_{m\neq 0}\left[\sum_a \frac{|(na|\rho_m)|^2}{\omega-\epsilon_a-\omega_m+i\eta}+\sum_i \frac{|(in|\rho_m)|^2}{\omega-\epsilon_i+\omega_m-i\eta}\right]. \tag{0.39}$$

Now we have the following definition,

$$
\begin{aligned}
&\rho_m(x)=\langle\Psi_0|\hat{\rho}(x)|\Psi_m\rangle \\
=&\sum_{bj}\langle\Psi_0|\hat{a}_j^\dagger\hat{a}_b|\Psi_m\rangle\phi_b(x)\phi_j^*(x)+\sum_{jb}\langle\Psi_0|\hat{a}_b^\dagger\hat{a}_j|\Psi_m\rangle\phi_j(x)\phi_b^*(x) \\
=&\sum_{bj}X_{bj}^m\phi_b(x)\phi_j^*(x)+\sum_{jb}Y_{bj}^m\phi_j(x)\phi_b^*(x) \\
=&\sum_{bj}\left(X_{bj}^m+Y_{bj}^m\right)\phi_b(x)\phi_j(x),
\end{aligned}
\tag{0.40}
$$

where for real orbitals the last equality holds. Thus

$$\begin{aligned}&\Sigma_c^{G_0W_0}(n,n;\omega)\\&=\sum_{m\neq 0}\left[\sum_a \frac{(na|\rho_m)^2}{\omega-\epsilon_a-\omega_m+i\eta}+\sum_i \frac{(ni|\rho_m)^2}{\omega-\epsilon_i+\omega_m-i\eta}\right],\end{aligned} \tag{0.41}$$

where the integrals are evaluated by the following expression,

$$(ns|\rho_m)=\sum_{bj}(ns|bj)\,(X+Y)_{bj}^m\,, \tag{0.42}$$

which scales as $O(N^4)$ for each excitation m. X_{bj}^m and Y_{bj}^m are the eigenvector components for the ph-RPA eigenvalue problem,

$$\begin{bmatrix}\mathbf{A} & \mathbf{B}\\ \mathbf{B}^* & \mathbf{A}^*\end{bmatrix}\begin{bmatrix}\mathbf{X}^m\\ \mathbf{Y}^m\end{bmatrix}=\omega_m\begin{bmatrix}\mathbf{X}^m\\ -\mathbf{Y}^m\end{bmatrix}, \tag{0.43}$$

where the matrix elements are given by

$$A_{ai,bj}=(\epsilon_a-\epsilon_i)\,\delta_{ab}\delta_{ij}+(ai|jb), \tag{0.44}$$

$$B_{ai,a'i'}=(ai|bj). \tag{0.45}$$

The chemists notation for the two-electron integral is defined as

$$(ai|bj)=\int dx_1dx_2\frac{\phi_a^*(x_1)\phi_i(x_1)\phi_b^*(x_2)\phi_j(x_2)}{|\mathbf{r}_1-\mathbf{r}_2|}, \tag{0.46}$$

Thus the evaluation of the integrals $(ns|\rho_m)$ is the computational bottleneck. Let us perform the resolution of identity,

$$\begin{aligned}
&(ns|\rho_m) \\
=&\sum_{bj}(ns|bj)\left(X+Y\right)_{bj}^{m} \\
=&\sum_{P}\sum_{bj}(ns|P)(P|bj)\left(X+Y\right)_{bj}^{m} \\
=&\sum_{P}(ns|P)(P|X+Y)^{m},
\end{aligned} \tag{0.47}$$

where P is an orthonormal basis. Thus the scaling for evaluating the integrals $(ns|\rho_m)$ for each excitation m is reduced to $O(N^3)$. The overall scaling is $O(N^5)$.

In fact for the particle-hole GW, it is not optimal to perform the diagonalization in order to obtain all the eigenvectors of the TDDFT equation because it scales unfavorably. Now if we choose χ to be the ph-RPA one, the following formula holds for the self energy,

$$\begin{aligned}
&\Sigma_c^{G_0W_0}(n,n;\omega) \\
=&-\sum_{p}\int\frac{d\omega'}{2\pi i}e^{-i\omega'\eta}\langle np|\bar{W}^{ph}(\omega')|np\rangle G_{pp}^{KS}(\omega-\omega') \\
=&-\int\frac{d\omega'}{2\pi i}e^{-i\omega'\eta}\left(\sum_{a}\frac{\langle na|\bar{W}^{ph}(\omega')|na\rangle}{\omega-\omega'-\epsilon_a+i\eta}+\sum_{i}\frac{\langle ni|\bar{W}^{ph}(\omega')|ni\rangle}{\omega-\omega'-\epsilon_i-i\eta}\right).
\end{aligned} \tag{0.48}$$

Now that for the ph-RPA approximation of χ, we have

$$\bar{W}^{ph}(\omega')=\bar{V}^{ph}+\bar{V}^{ph}\chi^{KS}(\omega')\bar{W}^{ph}(\omega'). \tag{0.49}$$

Thus

$$\bar{W}^{ph}(\omega')=\left[1-\bar{V}^{ph}\chi^{KS}(\omega')\right]^{-1}\bar{V}^{ph}. \tag{0.50}$$

Now using the resolution-of-identity technique,

$$\begin{aligned}
&\langle np|\bar{W}^{ph}(\omega')|np\rangle \\
=&\sum_{\mu\nu\mu'\nu'} \langle np|\bar{V}^{ph}|\mu\rangle \left[\left(\bar{V}^{ph}\right)^{-1}\right]_{\mu\nu} \langle \nu|\bar{W}^{ph}(\omega')|\nu'\rangle \left[\left(\bar{V}^{ph}\right)^{-1}\right]_{\nu'\mu'} \langle \mu'|\bar{V}^{ph}|np\rangle \\
=&\sum_{\nu\nu'} C_{np}^{\nu} \langle \nu|\bar{W}^{ph}(\omega')|\nu'\rangle C_{np}^{\nu'},
\end{aligned} \tag{0.51}$$

the task is to evaluate $\langle \nu|\bar{W}^{ph}(\omega')|\nu'\rangle$. Clearly

$$\left(\bar{V}^{ph}\right)_{\mu\nu} = \int dx_1 dx_2 P_\mu(x_1)\frac{1}{r_{12}}P_\nu(x_2), \tag{0.52}$$

$$1_{\mu\nu} = \int dx P_\mu(x)P_\nu(x), \tag{0.53}$$

$$\begin{aligned}
\chi^{KS}_{\mu\nu}(\omega') =& \int dx_1 dx_2 P_\mu(x_1)\chi^{KS}(x_1, x_2|\omega')P_\nu(x_2) \\
=&\sum_{ia} \int dx_1 dx_2 P_\mu(x_1)P_\nu(x_2) \\
&\left[\frac{\phi_a(x_1)\phi_i^*(x_1)\phi_a^*(x_2)\phi_i(x_2)}{\omega - (\epsilon_a - \epsilon_i) + i\eta} - \frac{\phi_i(x_1)\phi_a^*(x_1)\phi_i^*(x_2)\phi_a(x_2)}{\omega + (\epsilon_a - \epsilon_i) - i\eta}\right] \\
=&\sum_{ia} \langle ai|\mu\rangle\langle ai|\nu\rangle \left[\frac{1}{\omega - (\epsilon_a - \epsilon_i) + i\eta} - \frac{1}{\omega + (\epsilon_a - \epsilon_i) - i\eta}\right],
\end{aligned} \tag{0.54}$$

where

$$\langle ai|\mu\rangle = \int dx \phi_a(x)\phi_i(x)P_\mu(x). \tag{0.55}$$

The evaluation of $\chi^{KS}_{\mu\nu}(\omega')$ is $O(N_{ABF}^2 N_{occ} N_{vir})$, which is the slowest step. The matrix inversion costs only $O(N_{ABF}^3)$. The integration over ω' can be performed numerically with a given number of integration grid points.

The pp case

We now derive our new results connecting pp-RPA with T-matrix theory. For the pp case, there is the antisymmetry issue. The pp-RPA propagator equation is given by

$$\begin{aligned} K_{pq,rs}(\omega) =& K^{KS}_{pq,rs}(\omega) + \frac{1}{4}\sum_{p'q'r's'} K^{KS}_{pq,p'q'}(\omega)\langle p'q'|V^{pp}|r's'\rangle K_{r's',rs}(\omega) \\ =& K^{KS}_{pq,rs}(\omega) + \sum_{p'<q'}\sum_{r'<s'} K^{KS}_{pq,p'q'}(\omega)\langle p'q'|V^{pp}|r's'\rangle K_{r's',rs}(\omega), \end{aligned} \tag{0.56}$$

where in the second equality we used the antisymmetry of V^{pp} and K. Recalling that for the pp channel, we rewrite the first-order self energy as

$$\Sigma^{(1)}_{rs}(t_r - t_s) = (-1)i\sum_{r's'}\langle rr'|V^{pp}|ss'\rangle G^{KS}_{s'r'}(t_s - t_r)\delta(t_r, t_s^+), \tag{0.57}$$

containing the Hartree and Fock contributions. Also we have the pp four-point interaction (differing with the T matrix by a factor of -1)

$$\begin{aligned} &\langle rr'|W^{pp}(t_r - t_s)|ss'\rangle \\ =&\langle rr'|V^{pp}|ss'\rangle\delta(t_r, t_s^+) + \frac{1}{4}\sum_{uvu'v'}\langle rr'|V^{pp}|uv\rangle K_{uv,u'v'}(t_r - t_s)\langle u'v'|V^{pp}|ss'\rangle \\ =&\langle rr'|V^{pp}|ss'\rangle\delta(t_r, t_s^+) + \sum_{u<v}\sum_{u'<v'}\langle rr'|V^{pp}|uv\rangle K_{uv,u'v'}(t_r - t_s)\langle u'v'|V^{pp}|ss'\rangle, \end{aligned} \tag{0.58}$$

where in the third line we used the antisymmetry of V^{pp} and K. Therefore, the self energy is thus given by

$$\Sigma^{(1)}(r, s; ; t_r - t_s) = (-1)i\sum_{r's'}\langle rr'|W^{pp}(t_r - t_s)|ss'\rangle G^{KS}_{s'r'}(t_s - t_r), \tag{0.59}$$

whose Fourier transform is given by

$$\Sigma^{T}(r, s; \omega) = \sum_{r's'}\int \frac{d\omega'}{2\pi i}\langle rr'|W^{pp}(\omega + \omega')|ss'\rangle G^{KS}_{s'r'}(\omega'). \tag{0.60}$$

Also notice that

$$\int d(t_r - t_s) e^{i\omega(t_r - t_s)} \delta(t_r, t_s^+) = e^{i\omega\eta}. \tag{0.61}$$

Thus the first-order Hartree-Fock self energy is given by

$$\begin{aligned}
&\Sigma^{(1)}(r, s; \omega) = \sum_{r's'} \int \frac{d\omega'}{2\pi i} \langle rr'|V^{pp}|ss'\rangle G^{KS}_{s'r'}(\omega') e^{i(\omega+\omega')\eta} \\
=&\sum_{r's'} \langle rr'|V^{pp}|ss'\rangle \delta_{r's'} \int \frac{d\omega'}{2\pi i} \left[\frac{\theta(r' - F)}{\omega' - \epsilon_{r'} + i\eta} + \frac{\theta(F - r')}{\omega' - \epsilon_{r'} - i\eta}\right] e^{i(\omega+\omega')\eta} \\
=&\sum_{r'} \langle rr'|V^{pp}|sr'\rangle \int \frac{d\omega'}{2\pi i} \left[\frac{\theta(r' - F)}{\omega' - \epsilon_{r'} + i\eta} + \frac{\theta(F - r')}{\omega' - \epsilon_{r'} - i\eta}\right] e^{i(\omega+\omega')\eta} \\
=&\sum_{r'} \langle rr'|V^{pp}|sr'\rangle \theta(F - r') \\
=&\sum_{i} \langle ri|V^{pp}|si\rangle = \sum_{i} \langle ri||si\rangle = \sum_{i} \left[(rs|ii) - (ri|is)\right],
\end{aligned} \tag{0.62}$$

where the factor $e^{i(\omega+\omega')\eta}$ requires that the integration should be performed on the upper-half-plane.

Now let us examine the correlation part,

$$\begin{aligned}
&\Sigma^{T}_{c}(r, s; \omega) \\
=&\sum_{r's'} \int \frac{d\omega'}{2\pi i} \sum_{u<v} \sum_{u'<v'} \langle rr'|V^{pp}|uv\rangle K_{uv,u'v'}(\omega + \omega') \langle u'v'|V^{pp}|ss'\rangle G^{KS}_{s'r'}(\omega') \\
=&\sum_{u<v} \sum_{u'<v'} \sum_{r's'} \langle rr'|V^{pp}|uv\rangle \langle u'v'|V^{pp}|ss'\rangle \int \frac{d\omega'}{2\pi i} K_{uv,u'v'}(\omega + \omega') G^{KS}_{s'r'}(\omega').
\end{aligned} \tag{0.63}$$

Because

$$K_{uv,u'v'}(\omega) \tag{0.64}$$

$$= \sum_{m} \frac{\chi^{N+2,m}_{uv} \left(\chi^{N+2,m}_{u'v'}\right)^*}{\omega - \omega^{N+2}_{m} + i\eta} - \sum_{m} \frac{\left(\chi^{N-2,m}_{u'v'}\right)^* \chi^{N-2,m}_{uv}}{\omega - \omega^{N-2}_{m} - i\eta}, \tag{0.65}$$

where we defined

$$\chi_{uv}^{N+2,m} = \langle \Psi_0^N | \hat{a}_u \hat{a}_v | \Psi_m^{N+2} \rangle, \tag{0.66}$$

$$\left(\chi_{u'v'}^{N+2,m}\right)^* = \langle \Psi_m^{N+2} | \hat{a}_{v'}^\dagger \hat{a}_{u'}^\dagger | \Psi_0^N \rangle, \tag{0.67}$$

$$\left(\chi_{u'v'}^{N-2,m}\right)^* = \langle \Psi_0^N | \hat{a}_{v'}^\dagger \hat{a}_{u'}^\dagger | \Psi_m^{N-2} \rangle, \tag{0.68}$$

$$\chi_{uv}^{N-2,m} = \langle \Psi_m^{N-2} | \hat{a}_u \hat{a}_v | \Psi_0^N \rangle. \tag{0.69}$$

Therefore,

$$\begin{aligned}
&\Sigma_c^T(r,s;\omega) \\
=&\sum_{u<v}\sum_{u'<v'}\sum_{r'}\langle rr'|V^{pp}|uv\rangle\langle u'v'|V^{pp}|sr'\rangle \\
&\int\frac{d\omega'}{2\pi i}\left[\sum_m \frac{\chi_{uv}^{N+2,m}\left(\chi_{u'v'}^{N+2,m}\right)^*}{\omega+\omega'-\omega_m^{N+2}+i\eta} - \sum_m \frac{\left(\chi_{u'v'}^{N-2,m}\right)^*\chi_{uv}^{N-2,m}}{\omega+\omega'-\omega_m^{N-2}-i\eta}\right]\left[\frac{\theta(r'-F)}{\omega'-\epsilon_{r'}+i\eta}+\frac{\theta(F-r')}{\omega'-\epsilon_{r'}-i\eta}\right] \\
=&\sum_{u<v}\sum_{u'<v'}\sum_{r'}\langle rr'|V^{pp}|uv\rangle\langle u'v'|V^{pp}|sr'\rangle \\
&\left\{\sum_m \frac{\left(\chi_{u'v'}^{N-2,m}\right)^*\chi_{uv}^{N-2,m}\theta(r'-F)}{\omega-\omega_m^{N-2}+\epsilon_{r'}-i\eta} + \sum_m \frac{\chi_{uv}^{N+2,m}\left(\chi_{u'v'}^{N+2,m}\right)^*\theta(F-r')}{\omega-\omega_m^{N+2}+\epsilon_{r'}+i\eta}\right\} \\
=&\sum_{u<v}\sum_{u'<v'}\sum_{a}\langle ra|V^{pp}|uv\rangle\langle u'v'|V^{pp}|sa\rangle\sum_m \frac{\left(\chi_{u'v'}^{N-2,m}\right)^*\chi_{uv}^{N-2,m}}{\omega-\omega_m^{N-2}+\epsilon_a-i\eta} \\
+&\sum_{u<v}\sum_{u'<v'}\sum_{i}\langle ri|V^{pp}|uv\rangle\langle u'v'|V^{pp}|si\rangle\sum_m \frac{\chi_{uv}^{N+2,m}\left(\chi_{u'v'}^{N+2,m}\right)^*}{\omega-\omega_m^{N+2}+\epsilon_i+i\eta}.
\end{aligned} \tag{0.70}$$

Its diagonal elements are given by

$$\begin{aligned}&\Sigma_c^T(n,n;\omega)\\&=\sum_{u<v}\sum_{u'<v'}\sum_{i}\langle ni||uv\rangle\langle u'v'||ni\rangle\sum_{m}\frac{\chi_{uv}^{N+2,m}\left(\chi_{u'v'}^{N+2,m}\right)^*}{\omega-\omega_m^{N+2}+\epsilon_i+i\eta}\\&+\sum_{u<v}\sum_{u'<v'}\sum_{a}\langle na||uv\rangle\langle u'v'||na\rangle\sum_{m}\frac{\left(\chi_{u'v'}^{N-2,m}\right)^*\chi_{uv}^{N-2,m}}{\omega-\omega_m^{N-2}+\epsilon_a-i\eta}.\end{aligned}\tag{0.71}$$

Now define the following integrals,

$$\langle ni|\chi^{N+2,m}\rangle=\sum_{u<v}\langle ni||uv\rangle\chi_{uv}^{N+2,m}=\sum_{c<d}\langle ni||cd\rangle X_{cd}^{N+2,m}+\sum_{k<l}\langle ni||kl\rangle Y_{kl}^{N+2,m},\tag{0.72}$$

$$\langle\chi^{N+2,m}|ni\rangle=\sum_{u'<v'}\left(\chi_{u'v'}^{N+2,m}\right)^*\langle u'v'||ni\rangle=\sum_{c<d}\left(X_{cd}^{N+2,m}\right)^*\langle cd||ni\rangle+\sum_{k<l}\left(Y_{kl}^{N+2,m}\right)^*\langle kl||ni\rangle,\tag{0.73}$$

$$\langle na|\chi^{N-2,m}\rangle=\sum_{u<v}\langle na||uv\rangle\chi_{uv}^{N-2,m}=\sum_{c<d}\langle na||cd\rangle X_{cd}^{N-2,m}+\sum_{k<l}\langle na||kl\rangle Y_{kl}^{N-2,m},\tag{0.74}$$

$$\langle\chi^{N-2,m}|na\rangle=\sum_{u'<v'}\left(\chi_{u'v'}^{N-2,m}\right)^*\langle u'v'||na\rangle=\sum_{c<d}\left(X_{cd}^{N-2,m}\right)^*\langle cd||na\rangle+\sum_{k<l}\left(Y_{kl}^{N-2,m}\right)^*\langle kl||na\rangle.\tag{0.75}$$

whose construction is $O(N^4)$ for each given excitation m. $X_{cd}^{N\pm2,m}$ and $Y_{kl}^{N\pm2,m}$ are the eigenvector components of the pp-RPA matrix.

$$\begin{bmatrix}\mathbf{A}&\mathbf{B}\\\mathbf{B}^{\mathrm{T}}&\mathbf{C}\end{bmatrix}\begin{bmatrix}\mathbf{X}^{N\pm2,m}\\\mathbf{Y}^{N\pm2,m}\end{bmatrix}=\omega_m^{N\pm2}\begin{bmatrix}\mathbf{X}^{N\pm2,m}\\-\mathbf{Y}^{N\pm2,m}\end{bmatrix},\tag{0.76}$$

where the matrix elements are given by

$$A_{ab,cd}=(\epsilon_a+\epsilon_b)\,\delta_{ac}\delta_{bd}+\langle ab||cd\rangle,\tag{0.77}$$

$$B_{ab,kl}=\langle ab||kl\rangle,\tag{0.78}$$

$$C_{ij,kl} = -\left(\epsilon_i + \epsilon_j\right)\delta_{ik}\delta_{jl} + \langle ij||kl\rangle, \tag{0.79}$$

where we used the restrictions $a < b$, $c < d$, $i < j$ and $k < l$. $\omega_m^{N\pm 2}$ represents the pp-RPA eigenvalue, namely the double electron addition/removal energy. The antisymmetrized two-electron integral in the physicist's notation is defined as

$$\langle ab||cd\rangle = \langle ab|cd\rangle - \langle ab|dc\rangle, \tag{0.80}$$

where

$$\langle ab|cd\rangle = \int dx_1 dx_2 \frac{\phi_a^*(x_1)\phi_b^*(x_2)\phi_c(x_1)\phi_d(x_2)}{|\mathbf{r}_1 - \mathbf{r}_2|}. \tag{0.81}$$

Thus the correlation part of the self energy is given by

$$\begin{aligned} &\Sigma_c^T(n,n;\omega) \\ &= \sum_i \sum_m \frac{|\langle ni|\chi^{N+2,m}\rangle|^2}{\omega + \epsilon_i - \omega_m^{N+2} + i\eta} + \sum_a \sum_m \frac{|\langle na|\chi^{N-2,m}\rangle|^2}{\omega + \epsilon_a - \omega_m^{N-2} - i\eta}. \end{aligned} \tag{0.82}$$

The overall scaling is $O(N^6)$. This is the key result of our work.

Basis set convergence

Table 1: The computed HOMO IPs and LUMO EAs with respect to different basis sets.

Basis set	Method	HOMO IPs			LUMO EAs		
		LiH	F_2	H_2O	LiH	F_2	H_2O
aug-cc-pVDZ	HF	8.131	18.237	13.832	0.225	-1.504	-0.958
	2^{nd}-order	7.868	14.012	11.246	0.291	0.042	-0.787
	T-matrix	8.024	15.164	12.053	0.276	0.128	-0.811
cc-pVTZ	HF	8.134	18.139	13.731	0.050	-2.366	-3.563
	2^{nd}-order	7.933	14.270	11.465	0.161	-0.133	-3.025
	T-matrix	8.075	15.403	12.200	0.135	-0.020	-3.094
cc-pVTZ-DH[a]	HF	8.137	18.202	13.816	0.203	-0.078	-0.061
	2^{nd}-order	7.936	14.283	11.477	0.281	-0.075	-0.053
	T-matrix	8.078	15.443	12.264	0.263	-0.076	-0.054
aug-cc-pVQZ	HF	8.144	18.190	13.869	0.220	-1.545	-0.702
	2^{nd}-order	7.999	14.336	11.611	0.297	0.039	-0.563
	T-matrix	8.116	15.505	12.401	0.279	0.046	-0.585
Ref.[b]		7.90	15.70	12.62	0.34	-	-

a. The Dunning-Hay double Rydberg basis functions are added on top of the cc-pVTZ for F and O. For Li and H the Dunning-Hay diffuse basis functions are used instead.

b. The reference values are taken from[8].

Here we observe that the IPs are relatively less sensitive with respect to the basis set, and that the cc-pVTZ values are reasonably well converged (notice that the addition of the Dunning-Hay functions does not change the IPs in a significant way). However, for the EAs, the cc-pVTZ values are far from converged, and the addition of the Dunning-Hay functions changes the EAs qualitatively. The same was also in an earlier work on IP/EA computations with the ΔMBPT(2) method[9], where the IPs generally vary less with respect to basis set choice (within ˜ 0.1 eV), while the Dunning-Hay double Rydberg basis functions are needed to obtain more accurate EA values.

Tabulated numerical results

Table 2: Experimental and computed HOMO ionization potentials of small molecules. The experimental values are taken from[8]; the molecular structures from the G3 set[10,11]; the results of self-consistent GW (sc-GW) and the G_0W_0 with the HF (G_0W_0 (HF)) and PBE (G_0W_0 (PBE)) references from[12]: unless otherwise specified. The last two rows show the mean signed errors (MSEs) and the mean absolute errors (MAE) with respect to experimental data. (Unit: eV)

System	Expt./Ref.	HF	PBE	2^{nd}-order (HF)	2^{nd}-order(PBE)	T (HF)	T (PBE)	sc-GW	G_0W_0(HF)	G_0W_0(PBE)
H_2O	12.62	13.73	6.81	11.46	8.29	12.20	10.98	12.3	12.1	11.9
CH_3OH	10.96	12.22	6.08	10.21	6.86	10.77	9.27	10.7	10.8	10.5
Ethanol	10.64	11.99	6.04	10.08	6.55	10.58	8.93	-	-	10.57[c]
CH_4	14.35	14.82	9.43	14.09	12.23	14.26	13.37	14.1	14.4	14.4
Ethane	12.20	13.23	8.12	12.40	10.55	12.55	11.54	-	-	12.63[c]
Propane	11.51	12.59	7.66	11.67	9.76	11.82	10.72	-	-	12.05[c]
N_2	15.58	17.14	10.13	15.02	11.32	15.61	13.67	15.1	15.7	15.6
HF	16.12	17.48	9.14	14.63	11.22	15.56	14.35	16.0	15.6	15.7
NH_3	10.82	11.64	5.91	10.20	7.66	10.64	9.55	10.8	11.0	10.6
F_2	15.70	18.14	9.24	14.27	9.25	15.40	13.08	15.2	15.2	16.2
BF[a]	11.00[a]	11.05	6.77	11.07	9.97	10.96	10.27	-	-	11.49[c]
LiH	7.90	8.13	4.34	7.93	5.91	8.08	7.91	8.0	8.2	8.0
Ne	21.56	23.01	12.92	19.95	17.36	21.02	20.03	-	-	21.35[c]
CO	14.01	15.14	9.01	14.09	11.23	14.33	12.71	13.4	14.1	13.9
CO_2	13.77	14.74	8.97	13.05	10.11	13.49	11.89	13.1	13.3	13.6
C_2H_2	11.49	11.07	7.09	11.28	10.46	11.06	10.39	10.6	11.1	11.2
H_2CO	10.89	12.07	6.15	9.94	6.22	10.61	9.13	10.4	10.5	10.6
H_2O_2	11.70	13.08	6.05	10.23	6.40	11.05	9.25	11.0	11.1	11.1
HCN	13.61	13.30	8.86	13.56	12.55	13.31	12.65	12.7	13.2	12.4
N_2H_4	8.98	11.10	5.54	9.45	6.80	9.88	8.59	9.8	10.1	9.5
C_2H_4	10.68	10.24	6.70	10.32	9.36	10.16	9.46	9.8	10.4	9.6
HCl	12.77[b]	12.94	7.95	12.39	11.07	12.47	11.80	12.2	12.5	12.5
H_2S	10.50	10.46	6.23	10.15	9.02	10.15	9.53	9.8	10.1	9.9
ClF	12.77[b]	13.49	7.80	12.42	9.52	12.64	11.22	12.4	12.4	13.0
PH_3	10.59	10.46	6.58	10.28	9.25	10.24	9.60	9.9	10.3	10.0
SiH_4	12.82	13.23	8.52	12.82	11.32	12.89	12.11	12.3	12.6	12.4
MSE	-	0.807	-4.904	-0.483	-2.895	-0.146	-1.289	-0.430	-0.187	-0.187
MAE	-	0.910	4.904	0.560	2.895	0.313	1.290	0.518	0.364	0.408

a. Result and structure taken from[7].

b. Results taken from[13].

c. Results taken from[8].

Table 3: Experimental and computed LUMO EAs of small molecules. The reference values for the vertical EAs are taken from[8] for LiH, BH_3, NaCl and BN, and from[13] for CS_2, O_3, SO_2 and F_2; the molecular structures are from the G3 set[10,11] unless otherwise specified; two sets of reference G_0W_0 (PBE) results[8] are presented, one obtained with TURBOMOLE (TM-noRI) and the other with BerkeleyGW (BGW-GPP). The CCSD(T) results stand for the total energy differences between the N-particle system and the $(N+1)$-particle system, using the same basis set as in the T-matrix and the second-order self energy calculations. The last two rows show the mean signed errors (MSE) and the mean absolute errors (MAE) with respect to the reference data (left) and the CCSD(T) data (right). (Unit: eV)

System	Ref.	CCSD(T)	HF	2^{nd}-order(HF)	T(HF)	PBE	2^{nd}-order(PBE)	T(PBE)	G_0W_0(PBE)	
									TM-noRI	BGW-GPP
LiH	0.34	0.30	0.20	0.28	0.26	1.64	0.12	-0.08	0.07	0.37
BH_3[a]	0.04	-0.07	-0.08	-0.08	-0.08	3.06	1.01	-0.14	-0.12	0.06
NaCl	0.73	0.67	0.57	0.66	0.64	2.30	0.44	0.26	0.39	1.38
BN[b]	3.16	2.96	2.96	3.84	3.94	7.27	5.08	3.96	3.95	3.99
CS_2	0.01	-0.05	-0.06	-0.05	-0.05	2.85	1.01	0.64	0.20	0.43
O_3	1.93	1.81	1.62	1.93	2.80	6.38	3.25	1.91	2.30	2.59
SO_2	0.81	0.87	0.21	1.03	1.28	4.74	1.76	1.02	1.00	1.24
F_2	0.42	-0.07	-0.08	-0.08	-0.08	5.89	2.04	2.01	0.70	0.41
MSE	-	-	-0.262/-0.135	0.015/0.143	0.162/0.289	3.337/3.464	0.649/0.777	0.527/0.654	0.131/0.259	0.378/0.506
MAE	-	-	0.262/0.135	0.213/0.152	0.369/0.307	3.337/3.464	0.780/0.879	0.793/0.868	0.323/0.399	0.381/0.506

a. The bond length of the D_{3h} BH_3 was taken as 1.19 [14].

b. The bond length of BN was taken as 1.281 [15].

Table 4: Experimental and computed HOMO and core and ionization potentials of small molecules. The experimental values are taken from[16]. The last two rows show the mean signed errors (MSE) and the mean absolute errors (MAE) with respect to experimental data. (Unit: eV)

System	MO	Expt.	HF	2nd-order (HF)	T (HF)	PBE	2nd-order (PBE)	T (PBE)
Ne	$2p$	21.56	23.01	19.95	21.02	12.92	17.36	20.03
	$2s$	48.50	52.45	47.32	48.87	35.91	42.39	47.02
N_2	$3\sigma_g$	15.58	17.14	15.02	15.62	10.13	11.32	13.67
	$1\pi_u$	16.93	16.31	16.93	16.52	11.30	16.30	15.87
	$2\sigma_u$	18.75	21.46	18.34	19.32	13.63	12.52	16.62
	$2\sigma_g$	37.30	39.38	36.81	36.49	27.72	31.28	32.54
H_2O	$1b_1$	12.62	13.73	11.46	12.20	6.81	8.29	10.98
	$3a_1$	14.74	15.71	13.81	14.39	8.95	10.86	13.23
	$1b_2$	18.55	19.15	18.02	18.32	12.77	15.84	17.51
	$2a_1$	32.20	36.50	32.43	33.68	24.92	26.20	31.48
CO	5σ	14.01	15.14	14.09	14.33	9.01	11.23	12.71
	1π	16.91	17.13	16.21	16.44	11.61	14.10	15.67
	4σ	19.72	21.82	18.49	19.56	14.07	13.05	17.43
	3σ	38.30	40.99	38.84	37.62	28.96	30.30	29.71
C_2H_2	$1\pi_u$	11.49	11.07	11.28	11.06	7.09	10.46	10.40
	$3\sigma_g$	16.70	18.47	16.73	17.22	12.14	13.15	15.42
	$2\sigma_u$	18.7	20.88	18.69	19.37	14.04	13.69	17.13
	$2\sigma_g$	23.5	27.89	24.65	25.59	18.49	18.39	22.99
H_2CO	$2b_2$	10.9	12.07	9.94	12.07	6.15	6.22	9.13
	$1b_1$	14.5	14.40	13.87	14.40	9.89	10.90	13.21
	$5a_1$	16.1	17.61	15.02	17.61	10.85	10.52	13.95
	$1b_2$	17.0	18.75	16.56	18.75	12.05	11.36	15.54
	$4a_1$	21.4	23.73	21.43	23.73	15.76	15.65	19.98
Furan	$1a_2$	9.0	8.67	8.52	8.37	5.63	7.27	7.43
	$2b_1$	10.4	10.85	9.74	9.91	6.88	7.64	8.68
	$9a_1$	13.0	14.75	12.32	12.87	8.96	8.09	10.56
MSE		-	1.566	-0.457	0.008	-5.835	-4.384	-1.902
MAE		-	1.678	0.616	0.540	5.835	4.384	1.902

Table 5: Computed valence and core and ionization potentials of furan as used in the TOC. The experimental data are taken from[17].

MO	PBE	HF	T (HF)
$1a_2$	5.63	8.67	8.37
$2b_1$	6.88	10.85	9.91
$9a_1$	8.96	14.75	12.87
$8a_1$	9.69	15.44	13.40
$6b_2$	9.90	15.66	14.11
$5b_2$	10.88	16.57	14.91
$1b_1$	10.99	17.19	14.72
$7a_1$	13.33	20.13	17.94
$6a_1$	14.02	21.32	19.04
$4b_2$	14.82	21.98	19.59
$3b_2$	18.51	27.36	24.44

References

(1) Yang, W.; Mori-Sánchez, P.; Cohen, A. J. Extension of Many-Body Theory and Approximate Density Functionals to Fractional Charges and Fractional Spins. *J. Chem. Phys.* **2013**, *139*, 104114.

(2) van Aggelen, H.; Yang, Y.; Yang, W. Exchange-Correlation Energy from Pairing Matrix Fluctuation and the Particle-Particle Random-Phase Approximation. *Phys. Rev. A* **2013**, *88*, 030501.

(3) Martin, R. M.; Reining, L.; Ceperley, D. M. *Interacting Electrons - Theory and Computational Approaches*; Cambridge University Press, 2016; p 238.

(4) Strinati, G. Application of the Green's Functions Method to the Study of the Optical Properties of Semiconductors. *Riv. Nuovo Cimento* **1988**, *11*, 1–86.

(5) Onida, G.; Reining, L.; Rubio, A. Electronic Excitations: Density-Functional Versus Many-Body Green's-Function Approaches. *Rev. Mod. Phys.* **2002**, *74*, 601–659.

(6) Ke, S. H. All-Electron GW Methods Implemented in Molecular Orbital Space: Ion-

ization Energy and Electron Affinity of Conjugated Molecules. *Phys Rev. B* **2011**, *84*, 205415.

(7) van Setten, M.; Weigend, F.; Evers, F. The GW-Method for Quantum Chemistry Applications: Theory and Implementation. *J. Chem. Theory Comput.* **2012**, *9*, 232–246.

(8) van Setten, M. J.; Caruso, F.; Sharifzadeh, S.; Ren, X.; Scheffler, M.; Liu, F.; Lischner, J.; Lin, L.; Deslippe, J. R.; Louie, S. G. GW100: Benchmarking G0W0 for Molecular Systems. *J. Chem. Theory Comput.* **2015**, *11*, 5665–5687.

(9) Beste, A.; Álvaro Vázquez-Mayagoitia,; Ortiz, J. V. Direct Delta MBPT(2) Method for Ionization Potentials, Electron Affinities, and Excitation Energies Using Fractional Occupation Numbers. *J. Chem. Phys.* **2013**, *138*, 074101.

(10) Curtiss, L. A.; Raghavachari, K.; Redfern, P. C.; Rassolov, V.; Pople, J. A. Gaussian-3 (G3) Theory for Molecules Containing First and Second-Row Atoms. *J. Chem. Phys.* **1998**, *109*, 7764–7776.

(11) Curtiss, L. A.; Raghavachari, K.; Redfern, P. C.; Pople, J. A. Assessment of Gaussian-3 and Density Functional Theories for a Larger Experimental Test Set. *J. Chem. Phys.* **2000**, *112*, 7374.

(12) Rostgaard, C.; Jacobsen, K. W.; Thygesen, K. S. Fully Self-Consistent GW Calculations for Molecules. *Phys. Rev. B* **2010**, *81*, 085103.

(13) Lin, Y.-S.; Tsai, C.-W.; Chai, J.-D. Long-Range Corrected Hybrid Meta-Generalized-Gradient Approximations with Dispersion Corrections. *J. Chem. Phys.* **2012**, *136*, 154109.

(14) Kawaguchi, K. Fourier Transform Infrared Spectroscopy of the BH3 ν3 Band. *J. Chem. Phys.* **1992**, *96*, 3411–3415.

(15) Willock, D. J. *Molecular Symmetry*; John Wiley and Sons, 2009.

(16) Chong, D.; Gritsenko, O.; Baerends, E. Interpretation of the Kohn-Sham Orbital Energies as Approximate Vertical Ionization Potentials. *J. Chem. Phys.* **2002**, *116*, 1760–1772.

(17) Bieri, G.; Åsbrink, L.; von Niessen, W. 30.4-nm He (II) Photoelectron Spectra of Organic Molecules: Part VII. Miscellaneous Compounds. *J. Electron Spectrosc. Relat. Phenom.* **1982**, *27*, 129–178.